Structure of gap junctions in cultures of normal and neoplastic bladder epithelial cells[1]

B.U. Pauli and R.S. Weinstein

Department of Pathology, Rush Medical College, Chicago (Illinois 60612, USA), 31 July 1980

Summary. Normal rat urinary bladder epithelial cells contain small subunit (PF-1) and large subunit (PF-2) gap junctions, whereas carcinoma cells only contain PF-1 gap junctions. The absence of PF-2 gap junctions, which are composed of larger connexons with slightly larger ionic channels, may contribute to altered metabolic coupling between urinary bladder carcinoma cells.

In the Unwin-Zamphigi model[2], the gap junction is pictured as a bipartite array of units, called connexons[3], which receives equal structural contributions from each partner of the cell pair. The connexons are protein oligomers that span the lipid bilayer of the junctional membranes[4,5]. As seen in freeze-fracture replicas, connexons are often organized in densely packed hexagonal arrays[5], which are called PF-1 gap junctions[6]. PF-1 connexons have been described as cylinders composed of 6 subunits which surround a narrow central channel through the junctional membranes[2]. Mapping of connexons from PF-1 gap junctions by high resolution electron microscopic techniques has shown that the subunits, which tilt around the connexion axis, can exist in 2 configurations: an 'open' and a 'closed' pore configuration[2]. These alternate configurations may regulate the passage of small molecules between cell interiors[7]. It is widely believed that this direct transfer of small molecules from one cell to the other through open gap junctional channels may regulate such activities as tissue metabolism, growth, and differentiation[8]. Since these types of activities are frequently deranged in malignancies[9], we have examined the ultrastructure and configuration of gap junctions in an in vitro tumor model[10], using an in situ freeze-fracture technique[10,11]. Primary cultures of epithelial cells from normal Fischer rat urinary bladders[12] and carcinoma cells in long term cultures (passage 80), which we derived from non-invasive and invasive N-(4-(5-nitro-2-furyl)-2-thiazolyl)-formamide (FANFT)-induced rat urinary bladder tumors,

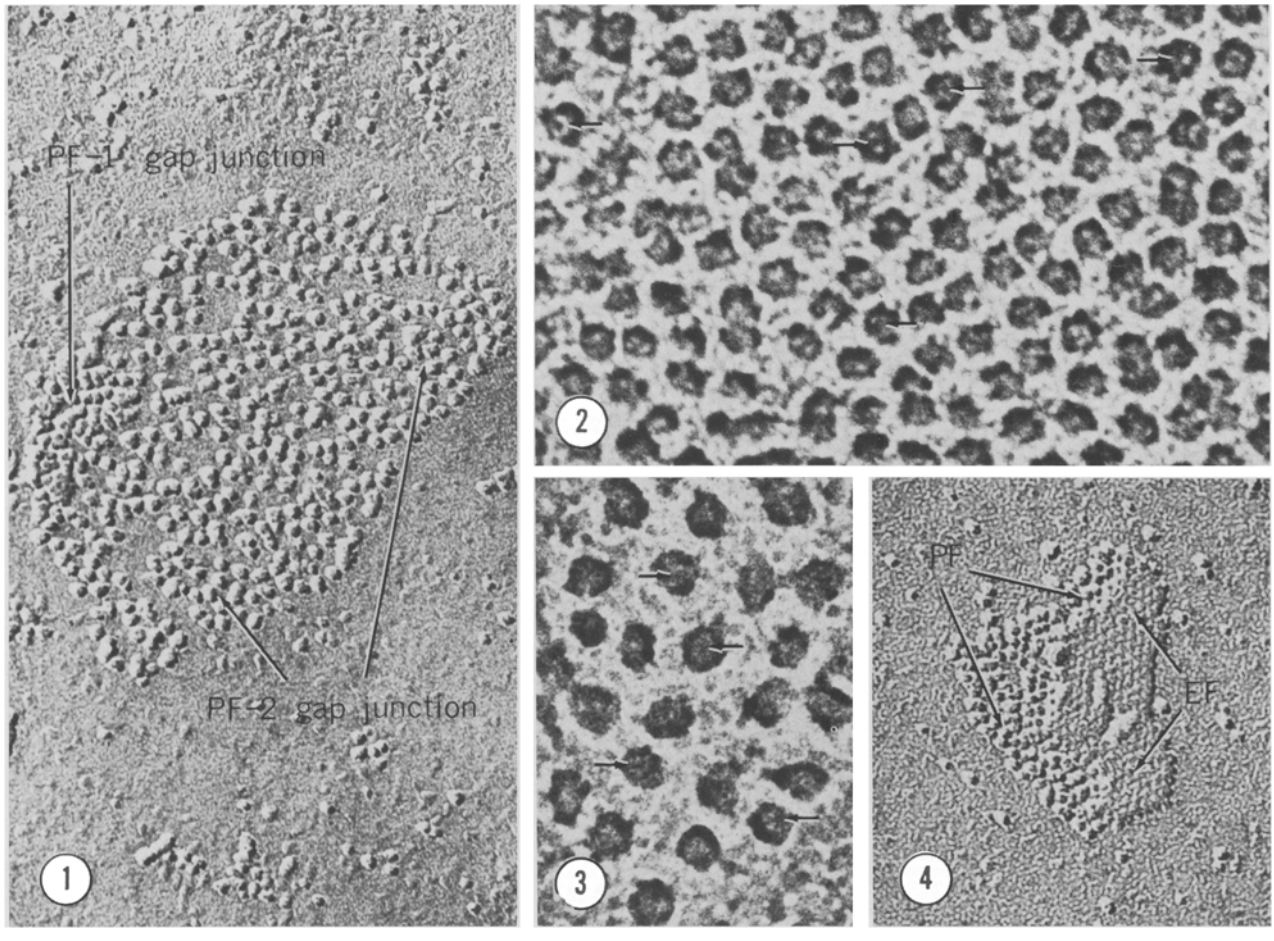

Fig. 1. Normal rat bladder epithelium in vitro contains PF-1 and PF-2 gap junctions in close proximity. Unidirectional shadowing: 45°. × 148,000. Fig. 2. PF-1 gap junction connexons of normal rat bladder epithelium consist of 6 globular 'subunits' that may appear in closed or open configurations. An open channel may be indicated by the presence of a dense metal core in the center of a freeze-fractured, rotary shadowed connexon (arrow). Rotary shadowing: 30°. × 550,000. Fig. 3. PF-2 gap junctions of normal rat bladder epithelium are composed of larger connexons (compare figure 1) with slightly wider ionic channels (arrow) than PF-1 gap junctions. Rotary shadowing: 30°. × 550,000. Fig. 4. A PF-1 gap junction of an invasive carcinoma cell consists of a hexagonal array of connexons (P-face) and corresponding pits (E-face). Unidirectional shadowing: 45°. × 112,000.

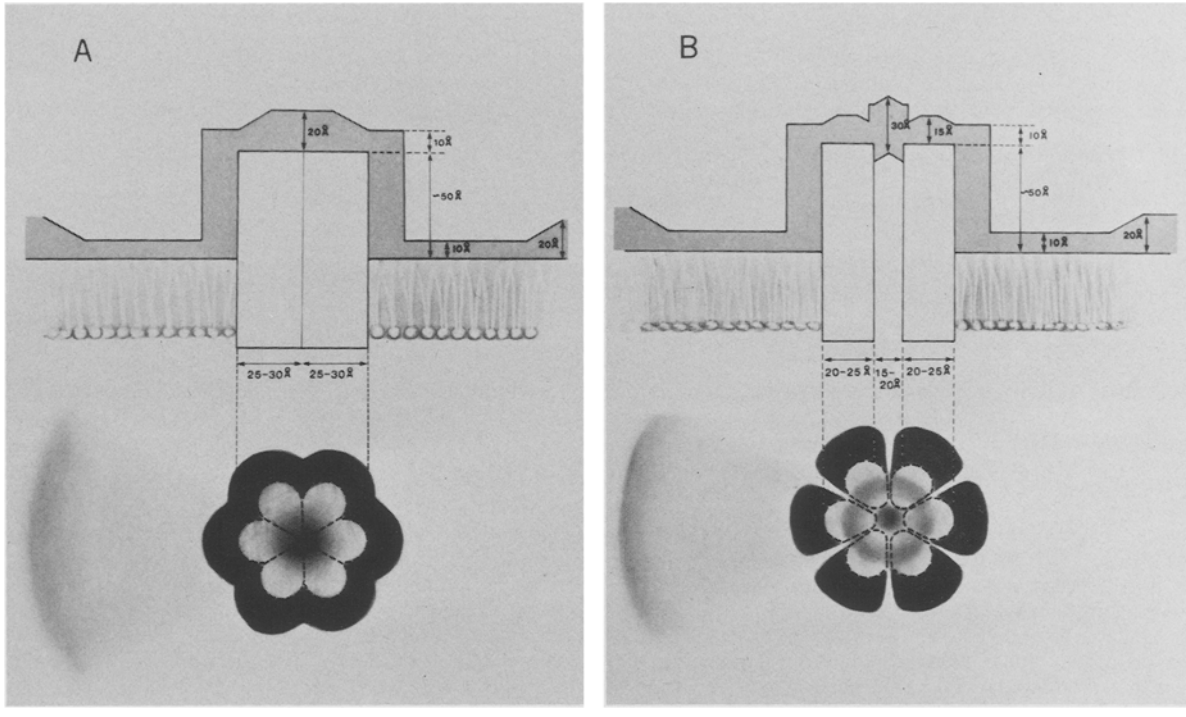

Chart. Rotary shadow replica of a gap junction connexon. *A* Connexon with closed ionic channel, *B* Connexon with open ionic channel. Each connexon consists of 6 cylindrical subunits that may appear in an open or closed configuration. The cylindrical subunit has a diameter of 20–25 Å and protudes about 50 Å from the protoplasmic membrane leaflet (PF). The extent of protusion has been calculated from the shadow angle and the shadow length. In the open configuration (B), the connexon shows a central metal core which has a diameter equal to that of the ionic channel, about 15 Å in PF-1 gap junctions and about 20 Å in PF-2 gap junctions.

were grown on Thermanox® plastic coverslips to confluency, and chemically fixed with buffered glutaraldehyde[10]. Monolayers were processed for freeze-fracture electron microscopy as previously described[10,11]. Replicas were prepared by both the standard unidirectional and the rotary shadow cast techniques[13].

Normal epithelial cell monolayers contained 2 types of gap junctions[4,6]. These 2 gap junction types were indentified by size and distribution of their intramembrane particles (IMP) in the P-face of the freeze-fractured plasma membrane (figure 1). In PF-1 junctions, IMP measured 6–7 nm in replica diameter and had a center-to-center spacing of 8–10 nm. The IMP of PF-1 gap junctions were frequently in hexagonal arrays. The E-face membrane of PF-1 gap junctions displayed arrays of pits which had housed the junctional IMP prior to the fracturing procedure. The PF-2 gap junction, consisted of irregular arrays of clustered IMP, which measured 10–11 nm in replica diameter and had a center-to-center spacing of greater than 20 nm.

In replicas prepared by the rotary shadow technique[13], both PF-1 and PF-2 gap junctions contained 2 ultrastructurally distinctive populations of IMP. One population displayed a central, electron-lucent zone which was surrounded by a hexagonal array of 6 electron-dense globules (figure 2; chart, 1A). These globules represented the metal caps of rotary shadowed, rod-shaped subunits of the cylindrical gap junction IMP or connexon[2,3,5]. The 2nd population of rotary shadowed connexons had a similar ultrastructure, but in addition contained a central electron-dense core measuring approximately 15 A in diameter in PF-1 connexons (figure 2) and approximately 20 A in diameter in PF-2 connexons (figure 3). The electron dense core corresponded to the pore region of the connexon, where platinum accumulated during rotary shadowing (chart, B). Analogous structures were previously visualized in uni-directionally shadowed PF-1 gap junctions[4], but are seen to better advantage with rotary shadowing. Theoretically, the apparent pore diameter in rotary shadowed replicas should approximate the true pore diameter, which is consistant with data obtained with other methods[2]. We postulate that the connexons with the electron dense centers may have an open ionic channel, whereas those lacking this structure may have a closed channel, as shown recently in the model of Unwin and Zampighi[2].

Non-invasive and invasive carcinoma cells isolated from FANFT-induced tumors contained many normal appearing PF-1 gap junctions (figure 4), but were devoid of PF-2 gap junctions. The absence of the PF-2 gap junctions, which are composed of larger connexons with slightly larger ionic channels, may alter metabolic coupling between carcinoma cells[14]. It is therefore suggested that altered sieving properties between rat urinary bladder carcinoma cells may be responsible for such culture characteristics as non-contact-inhibited growth, the smaller PF-1 channels being insufficient in the transfer of growth controlling molecules between cell interiors.

These culture systems should be useful for studying the factors which influence the formation of gap junctions in epithelia during malignant transformation, as well as metabolic coupling between carcinoma cells.

1 Acknowledgments. The authors wish to thank Ms Denise Wiler and Mr William Leonard for expert technical assistance. This work was supported by funds from the National Cancer Institute, CA-25034, and in part by the Otho SA Sprague Memorial Institute.

2 P.N.T. Unwin and G. Zampighi, Nature *283*, 545 (1980).
3 D.A. Goodenough, J. Cell Biol. *68*, 220 (1976).

4 N.S. McNutt and R.S. Weinstein, Prog. Biophys. molec. Biol. *26*, 45 (1973).
5 J.D. Robertson, J. Cell Biol. *19*, 201 (1963).
6 L.A. Staehelin, Proc. natl Acad. Sci. *69*, 1318 (1972).
7 W.R. Loewenstein, Cold Spring Harb. Symp. quant. Biol. *40*, 49 (1975).
8 E.B. Griepp and J.P. Revel, in: Intercellular Communication, p. 1. Ed. W.C. De Mello Plenum Press, New York 1977.
9 R.S. Weinstein, F.B. Merk and J. Alroy, Adv. Canc. Res. *23*, 23 (1976).
10 B.U. Pauli, K.E. Kuettner and R.S. Weinstein, J. Microsc. *115*, 271 (1978).
11 B.U. Pauli, R.S. Weinstein, L.W. Soble and J. Alroy, J. Cell Biol. *72*, 763 (1977).
12 B.U. Pauli, S.N. Anderson, V.A. Memoli and K.E. Kuettner, Cell Tissue, in press (1981).
13 L.HJ. Margaritis, A. Elgsaeter and D. Branton, J. Cell Biol. *72*, 47 (1977).
14 R. Azarnia and W.R. Loewenstein, J. Membrane Biol. *30*, 175 (1976).

Anthelmintic activity of several 5-substituted benzimidazolyl carbamates against *Hymenolepis nana* cysticercoids

Marie Novak and B.J. Blackburn

Departments of Biology and Chemistry, University of Winnipeg, Winnipeg (Manitoba, Canada R3B 2E9), 29 May 1980

Summary. Several benzimidazolyl carbamate derivatives effective against *Hymenolepis nana* cysticercoids were found.

There is still today a scarcity of anthelmintics which are effective against larval tapeworms. In recent years a number of benzimidazole derivatives with promising anthelmintic properties have been discovered. Among these, 5-substituted benzimidazolyl carbamates have been found active in preventing, inhibiting and curing various metacestode infections[1-7]. Here we report the discovery of additional 5-substituted benzimidazolyl carbamate derivatives with cestocidal properties (table). All compounds were synthesized in our laboratory[8]. Three of them (II, IV and V) have been made for the first time, and their synthesis and properties will be published elsewhere. The 2 remaining compounds (I and III) have been synthesized before by a somewhat different method[9], but were never tested against cestodes.

To test these compounds for anthelmintic activity we used the *Tribolium confusum* - *Hymenolepis nana* system. The flour beetles infected with *H. nana* eggs were fed continuously from day 1 to day 10 post infection on mixtures of 9 parts flour and 1 part drug, the concentration used previously[2,3] in studies with mebendazole, another benzimidazolyl carbamate. Control beetles received only four.

On day 10 post infection the beetles fed compounds I, II, III and IV contained significantly ($p < 0.001$) fewer postoncosphere stages than the controls. Also, whereas all the parasites in the control beetles had become fully developed cysticercoids, many of those in the drug-treated groups were retarded. This inhibiting effect varied with the drug tested. The most potent drug proved to be compound I where all the parasites (100%) failed to reach the fully developed cysticercoid stage, followed by compounds II, III, IV and V with decreasing potency in that order. Haemocoel contents of hosts treated with compounds I, II, III and IV contained in addition to the various postoncospheral stages many oncospheres that were alive but had not progressed beyond this stage of development. Their presence indicated that these compounds, though they drastically arrested the development of larvae, did not kill them. No oncospheres were found in control beetles or beetles fed compound V. The mean number of postoncospheral stages in beetles fed compound V was comparable to those in the controls ($p > 0.05$), yet 17% of them were underdeveloped larvae, suggesting the weak, but still noticeable effect of this drug. None of the compounds tested caused beetle mortality.

Thus the results with the first 4 compounds presented here are comparable to those reported for *H. nana* and mebendazole[2,3,6].

Although the larval stages of *H. nana* seem to have some resistance to benzimidazolyl carbamates, it is known that the adults of this parasite are easily expelled by mebendazole from the intestinal lumen of mice[6] and humans[7]. It is reasonable then to assume that the compounds reported here might also be useful against *H. nana* in man.

Unlike hymenolepidid larvae, metacestodes such as *Echinococcus multilocularis*, *E. granulosus*, *Taenia crassiceps*, *T. pisiformis* and *Mesocestoides corti* are highly susceptible to treatment with many benzimidazoles[1,4,5]. Therefore the compounds presented in this study should also be tested for possible activity against other larval cestodes.

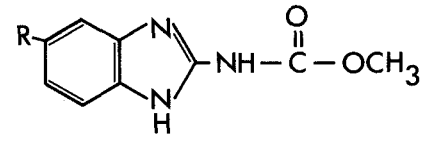

Compound	R	Mean number postoncosphere stages per beetle (± SE)*	p	Total number postoncosphere stages	Underdeveloped stages (%)	Fullydeveloped cysticercoids (%)
Control	No treatment	17.40 ± 1.19	-	1035	0	100
I	$-Cl$	0.54 ± 0.12	< 0.001	35	100	0
II	$-OCH_3$	0.26 ± 0.07	< 0.001	17	88	12
III	$-CH_3$	0.81 ± 0.25	< 0.001	56	73	27
IV	$-NO_2$	6.87 ± 1.20	< 0.001	482	32	68
V	$-CO_2H$	18.37 ± 1.34	> 0.05	1182	17	83

* Summarized results from 3 replicate experiments. All groups contained 25 beetles when the experiments began and at least 20 live beetles at day 10 post infection when the experiments were terminated.